

Review

Moving Towards a Network of Autonomous UAS Atmospheric Profiling Stations for Observations in the Earth's Lower Atmosphere: The 3D Mesonet Concept

Phillip B. Chilson^{1,†,‡}, Fred Carr¹, Christopher Fiebrich^{1,‡}, Mark Yeary¹, Robert Huck¹, Keith Brewster¹, Elizabeth Pillar-Little¹, Robert D. Palmer¹, Mark Weber¹, Kenneth Carson¹, Jorge Salazar-Cerreno¹, Brian Greene¹, Tyler Bell¹, Antonio R. Segales¹, Gustavo Britto Hupsel de Azevedo¹, Sai Teja Kanneganti¹, William Doyle¹, James Grimsley¹, Joshua Martin¹, Brent Wolf¹, and Kelvin Droegeemeier¹,

¹ Affiliation 1; e-mail@e-mail.com

² Affiliation 2; e-mail@e-mail.com

* Correspondence: chilson@ou.edu; Tel.: +1-405-325-5095

† Current address: Affiliation 3

‡ These authors contributed equally to this work.

Academic Editor: name

Version December 10, 2018 submitted to Sensors; Typeset by L^AT_EX using class file mdpi.cls

1 **Abstract:** The deployment of small unmanned aircraft to collect in-situ vertical measurements
2 of the atmospheric state in conjunction with other meteorological observations has the potential
3 to significantly expand our weather observation capabilities. We briefly report on a concept of
4 adding the capability of collecting vertical atmospheric measurements (profiles) through the use
5 of unmanned aerial systems (UAS) at sites deemed suitable for this application. The system must
6 be able to operate unattended, which necessitates the inclusion of risk mitigation measures such
7 as detect and avoid radar and the ability to transmit and receive transponder signals. It is also
8 necessary for the system to be capable of assessing local weather conditions (visibility, surface winds,
9 cloud height) and the integrity of the vehicle (system diagnostics, fuel level) before takeoff. We begin
10 by providing a notional concept of operations for a 3D Mesonet and a description of the technical
11 configuration for one such station in the network. We then report on progress being made to develop
12 and test a prototype 3D Mesonet station and show preliminary measurements and discuss how such
13 measurements from an operational network could be utilized to better characterize the atmospheric
14 boundary layer, improve weather forecasts, and help to identify threats of severe weather.

15 **Keywords:** keyword 1; keyword 2; keyword 3. List three to ten pertinent keywords specific to the
16 article, yet reasonably common within the subject discipline.

17 1. Introduction

- 18** • Discuss the complexity of the atmospheric boundary layer (ABL) and the importance of
19 monitoring and modeling this region
- 20** • Difficulty in acquiring adequate and quality measurements with conventional instrumentation in
21 the ABL
- 22** • Provide a graphic of the ABL (Figure 1)
- 23** • Recommendations from NAS, NRC, NCAR, NSF, etc to collect more data in the ABL
- 24** • Growing development of UAS for atmospheric measurements and how this could fill the
25 measurement gap

- 26 • Briefly introduce the 3D Mesonet Concept
- 27 • How these observations could impact weather forecasting and more
- 28 • Layout the paper structure

29 Dramatic, high-impact weather events, such as severe thunderstorms with hail and wind,
30 tornadoes, excessive rainfall and flooding, tropical storms, ice storms, heavy snowstorms, and
31 blizzards have an impact of billions of dollars per year on the economy of the United States [1,2].
32 Additionally, a number of industries in the US are quite weather sensitive, including agriculture,
33 transportation and electric power generation and management. Definitive links are being made
34 between climate change and the impact it is having on the occurrence of dramatic weather events
35 [3]. To mitigate deleterious impacts on society and its infrastructure, it is imperative that we develop
36 innovative means of monitoring and modeling the Earth's atmosphere. To achieve this end, we
37 require better observations of the lower atmosphere and an effective means of incorporating these
38 measurements into numerical weather predictions. That is, the availability of quality atmospheric
39 observations is critical to our ability to monitor meteorological conditions and accurately forecast the
40 weather.

41 Meteorological observations fall largely into two categories: in-situ and remote sensing. The
42 former involves the measurement by instruments, which are directly exposed to the atmosphere. In
43 this case, continual observations of the atmosphere are limited to sensors, which can be placed at
44 or near the Earth's surface (e.g., using instrumented towers). To obtain in-situ measurements aloft,
45 balloons, kites, or aircraft must be used. Sensors capable of remotely probing the Earth's atmosphere,
46 such as radar, are capable of providing continual observation. However, the number of atmospheric
47 parameters such technologies can provide is limited and the data often must be inferred from other
48 measured quantities (e.g., radar reflectivity). For example, rainfall rates provided by weather radar
49 are estimated based on the strength of the backscattered signal from the precipitation.

50 A long-desired component to the U.S. operational observing systems is the capability to measure
51 vertical profiles of wind, temperature and moisture in the lower troposphere at high spatial and
52 temporal resolution. Sounding data can be used to assess regions of thermal stratification and
53 the degree of atmospheric static and dynamic stability. Overall, processes in the PBL can vary
54 dramatically over a single diurnal cycle as depicted in Figure 1. Although this conceptual model
55 of the PBL is idealized, it helps to illuminate several common features of the PBL structure: mixed
56 layer, capping and nocturnal inversion, the surface layer, the residual layer, and so forth. To fully
57 characterize the PBL, measurements of the state parameters in each of these regions are needed,
58 preferably with adequate temporal resolution to fully capture evolution of the height of the PBL and
59 structures within the PBL.

60 This need is reflected in several recent studies, some of which provide explicit recommendations
61 to collect more observations within the atmospheric boundary layer (ABL), in general with a focus on
62 vertical sampling (profiling) in particular [4–8]. These reports emphatically state that our currently
63 available observing systems are not capable of providing adequately detailed profiles of temperature,
64 moisture, and winds within the ABL. Height profiles of virtual potential temperature can be used
65 to identify regions of thermal stratification and the degree of atmospheric stability. Moreover,
66 vertical wind shear is capable of producing turbulence and thus turbulent fluxes in the ABL. Overall,
67 processes in the ABL can vary dramatically over a single diurnal cycle. A depiction of the structure
68 of the ABL during a typical diurnal cycle is provided in Figure 1.

69 To address these considerations, advance several key recommendations listed in the NASA
70 Science Plan, and fulfill the mandates put before NOAA in the 2017 Weather Research Innovation
71 Act, we must challenge ourselves to develop observing and modeling systems that transcend the
72 conventional methods. An emerging technology, which could have dramatic impacts on observations
73 of the lower atmosphere, is that of Unmanned Aircraft Systems (UAS). It has been suggested that
74 such profiling could be done by small unmanned aerial vehicles (UAVs) assuming that autonomous
75 flights extend at least through the depth of the boundary layer [9]. As outlined below, instrumented

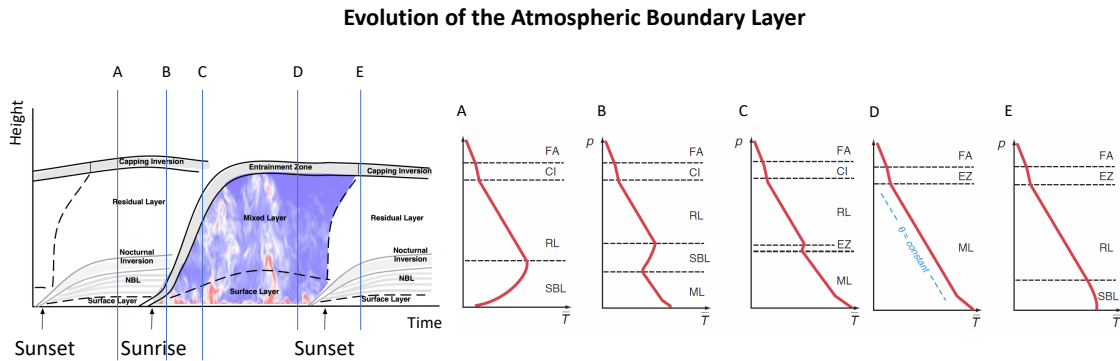


Figure 1. Schematic depicting the idealized structure of the PBL (left) during one diurnal cycle under quiescent conditions. Vertical profiles of the temperature at five particular times (denoted as A-E) are presented to the right. In this cloud-free example, the structure of the PBL is primarily driven by thermal forcing produced by insolation. [Modify figure or use Tyler's figure.](#)

76 UAS are expected to provide inexpensive, accurate, controlled, observations of the lower atmosphere.
 77 The advent of weather-observing UAS (WxUAS) would complement other observing systems,
 78 such as rawinsondes, towers, satellite-based remote sensors, and active and passive ground-based
 79 remote sensors. The true value of WxUAS lies in their ability to fill data gaps that conventional
 80 instrumentation cannot easily or feasibly provide, for example in the PBL.

81 **Reword this.** In recent decades, numerous states have established networks of *in-situ*
 82 meteorological observing stations (i.e., Mesonets) to aid decision making across various sectors
 83 ranging from emergency management to agriculture to weather forecasting to transportation [10,
 84 11]. In general, Mesonets aim to provide multi-purpose, high-quality, real-time observations.
 85 Additionally, they provide tailored outreach (typically to the K-12, university, public safety, and
 86 agriculture communities) to expand the utility of the observations. Across the United States, there
 87 are currently 27 statewide networks of mesoscale in situ meteorological observations (i.e., Mesonets;
 88 [10]). These networks range in size from less than 10 stations to over 175 stations, but each have a
 89 goal of providing high resolution observations to support mesoscale weather and climate monitoring.
 90 Typically, mesonets include sensors mounted on or below a 10 m tower to sample air temperature,
 91 relative humidity, winds, solar radiation, precipitation, pressure, and soil temperatures and soil
 92 moisture.

93 **Reword this and work in an introduction of the 3D Mesonet.** Typical Mesonet stations are
 94 located in areas that have minimal slope and minimal obstructions that impede environmental
 95 fetch. Ziokowska *et al.* [11] documented the value of mesonet data to many diverse sectors across
 96 Oklahoma, including those in agriculture, drought and climate monitoring, public safety, wildland
 97 fire management, nowcasting, and energy management. Mesonet observations are increasingly
 98 being used in forecast model development and in understanding land-atmosphere interactions. Both
 99 Mahmood *et al.* [10] and Ziokowska *et al.* [11] note that expanding Mesonet observations into the
 100 boundary layer via UAVs are an important next step to bring added value to sectors that could benefit
 101 from improved weather forecasts.

102 In addition to capturing the vertical structure of the PBL, WxUAS can be used to detect complex
 103 mesoscale features embedded in weather systems. In Figure 2, we present an example of the
 104 surface mesoscale wind and humidity field across Oklahoma on the afternoon of 26 March 2018.
 105 A combination of varying insolation across the state and the action of a cold front, dryline, and
 106 upper-level jet resulted in significant county-by-county variability. The implications of such features
 107 on wildfire risk (including likelihood for initiation, behavior, and smoke dispersion), convective
 108 initiation, and moisture and momentum fluxes are immense, yet inadequately understood without

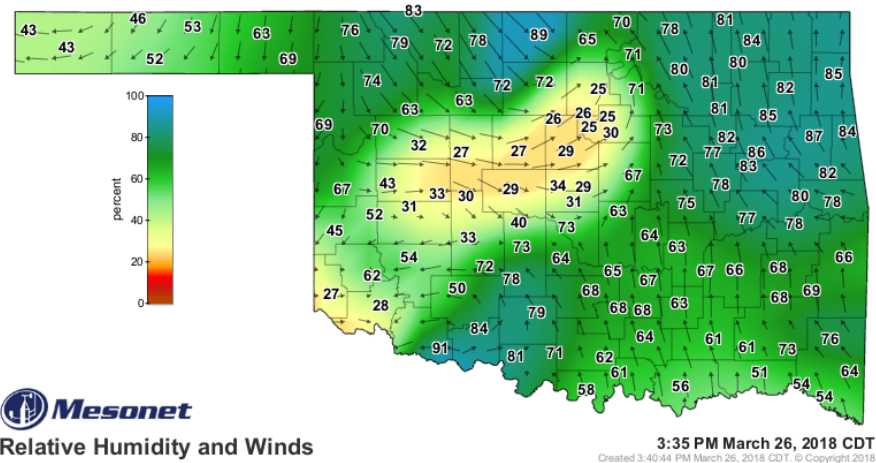


Figure 2. Mesonet station plot of relative humidity (%) and wind field streamlines across Oklahoma during the afternoon of 26 March 2018.

additional measurements of the PBL. It is difficult to underestimate the impact that additional mesoscale, 4D observations could have on detecting and predicting these phenomena.

As illustrated in Figure 2, the atmospheric surface layer can exhibit remarkably complex spatial structure in the wind and moisture fields. Moreover, the evolution of these structures over time can be equally complex. Even with observations from dense surface sensor networks, such as the Oklahoma Mesonet, the vertical structure remains unknown, so forecasters must rely on statistically-based parameterization schemes [12] and basic conceptual models to envision processes acting in the vertical dimension. Tremendous value would be added if the measurements depicted in Figure 2 could be extended vertically through the depth of the PBL. Providing researchers and forecasters with data that allow them to monitor the changing 4D wind, temperature and moisture patterns would yield considerable benefits. For example, subtle changes in the strength of the capping inversion can have a profound impact on the probability of convective initiation and the chance that storms may become severe. Further, these data can be used to initialize mesoscale and thunderstorm-scale NWP. Knowing if, when, and where the cap might “break” is paramount to anticipating where convection could be initiated. Current parameterization schemes struggle to provide adequate information on the strength of the capping inversion, mostly due to lack of observational data.

Provide a layout of the paper

2. Overview of the 3D Mesonet Concept

2.1. Growth of WxUAS

- Before launching into the 3D Mesonet, we provide a brief introduction to the growth and development of UAS for atmospheric measurements and weather observations (WxUAS)
- Discuss why we are currently witnessing growth in the area of UAS in general and WxUAS in particular
- Point out the growing interest in WxUAS as witnessed in professional societies: ISARRA and special sessions at AMS, AGU, AIAA
- WxUAS is transitioning from “toys to tools”

There has been rapid development in WxUAS technology and its integration into meteorological research for atmospheric boundary layer studies (Reuder et al., 2009; Martin et al., 2011, Wildmann et al., 2014). Much of the initial studies with WxUAS were conducted using fixed-wing aircraft. An overview paper of these platforms can be found in Elston et al., 2015). More recently, rotary-wing

139 vehicles are playing a prominent role in WxUAS research (e.g., Brosy et al., 2017; Hemingway et al.,
140 2017; Lee et al., 2017). Overwhelmingly, the WxUAS presented in the current literature are one-off
141 units developed by a research group for specific applications.

142 Currently there are no small unmanned aircraft systems which offer all measurement and
143 telemetry capabilities envisioned for autonomous operation. The proposed modular system will
144 allow for customization, upgrade, and in-field replacement of sensor packages as desired. Such a
145 system would facilitate off-site maintenance and calibration and would provide the ability to add
146 new sensors as they are developed, or as new requirements are identified. The small WxUAS must be
147 capable of handling the weight of all sensor packages and have lighting, communication, and aircraft
148 avoidance systems necessary to meet existing or future FAA regulations. The system must be able to
149 operate unattended or with remote piloting at such time that FAA regulations allow.

150 **Expand upon this and discuss how UAS is evolving from toy to tool.**

151 **2.2. Conceptual Framework of the 3D Mesonet**

- 152 • Pitch the 3D Mesonet concept
- 153 • Discuss how this might look when deployed across a broad footprint
- 154 • Provide a graphic of the 3D Mesonet concept (Figure 3)
- 155 • Need for unattended operations mandates:
 - 156 – Hardened UAVs with robust sensor units, which require minimal servicing and calibration;
 - 157 – Detect and avoid radar unit
 - 158 – ADS-B in & out capability
 - 159 – Ability to conduct internal diagnostics of the UAV and sensors
 - 160 – Video monitoring
 - 161 – Autonomous charging
 - 162 – Two-way communications between UAV (with data feed) and a central control unit
- 163 • A prototype is being deployed at the Kessler Atmospheric and Ecological Field Station

164 **Introduce the Center for Autonomous Sensing and Sampling (CASS) in this disussion.**

165 The miniaturization and maturation of technology has progressed to the point where
166 autonomous formations of small suborbital platforms, small Unmanned Aircraft Systems (sUAS),
167 can be confidently deployed to collect spatiotemporal atmospheric measurements related to
168 thermodynamic and kinematic state variables, particulate matter, and chemical components, which
169 are critical to the understanding of planetary boundary layer (PBL) processes integral to air-surface
170 (land, ocean and sea ice) exchanges of energy, momentum and mass; how these are affected by climate
171 variability; and how they impact weather forecasts and air quality simulations. We assert that robust
172 4D datasets collected using instrumented sUAS together with appropriate modeling approaches will
173 help address several of the most-important questions identified in the 2017-2027 Decadal Survey.

174 **2.3. Impact of Data on Weather Forecasting**

- 175 • Overview the philosophy & use of Observation System Simulation Experiments
- 176 • Discuss how our OSSE was set up
- 177 • Provide some results (we need to hold back because Andrew will include this in his paper)

178 **Still stitching this together.** The PBL largely provides the moisture, instability, low-level wind
179 shear, and forcing necessary for the formation of severe storms with attendant tornadoes, hail, and
180 hazardous winds. Within the PBL resides the storm-generated outflows that can regulate the strength
181 and longevity of severe storms or even trigger new storms. Knowledge of these conditions is the key
182 to improving predictions of severe weather events. The problem is that PBL properties are highly
183 variable on mesoscale time and space scales, which are virtually undetected by operational observing
184 systems.

185 It has been well established that shear in the near-ground layer is critically important for
186 distinguishing tornadic from nontornadic supercells and that traditional observational data, such

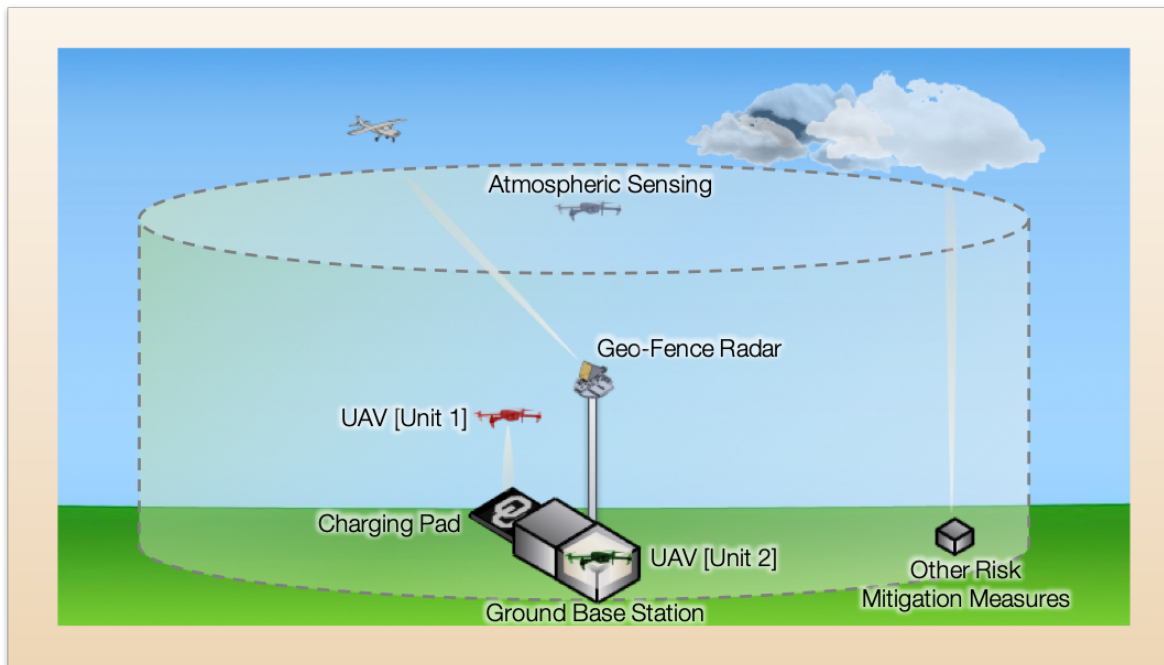


Figure 3. Placeholder: Graphic of the 3D Mesonet Concept. [Get original from Jorge or Arturo.](#)

as those provided by wind profiling radars do not provide adequate vertical resolution to resolve the shear [e.g., 13]. The most noticeable difference between nontornadic and tornadic cases is in the lower-tropospheric wind profile; specifically the orientation of the 0–500 m shear vector with respect to the storm-relative inflow. This implies that the tornadic cases have much more streamwise horizontal vorticity in the lowest 500 m AGL [14]. Traditional standards used for radiosonde data processing do not capture features in the lowest 500 m well. Therefore, there is a need to sample the PBL near the surface with finer vertical resolution.

Since FAA permission has not yet been granted to test such an observing network, the potential improvement that a UAV network could have on storm-scale numerical weather prediction using an Observation System Simulation Experiment (OSSE) approach. An OSSE is performed over the state of Oklahoma in which it is assumed that a UAV could be launched from 110 Oklahoma Mesonet [15] stations every hour, fly vertically to an assigned maximum altitude and return to its charging station, providing soundings at a roughly 35 km horizontal resolution. A case study of convective initiation (CI) was chosen for this study as a compromise between a fair-weather day and one with extensive ongoing convection. The OU ARPS [16] model provides a nature run at high (1 km) resolution, while the control run and OSSE experiments are done with the WRF-ARW model at 3 km. To simulate the effect of data from dozens of observing systems already included in operational models, the nature run data volume is sampled at synoptic scales and inserted into the control run via a 6-hr data assimilation (DA) period. Simulated hourly UAV temperature, moisture and wind data, with expected errors, are then added to the DA, followed by 12-hr forecasts. The analyses and forecasts are examined to assess the added value of UAV data. Tests are run to measure the impact of varying the maximum UAV altitude and the spatial density of UAV observations.

Initial results clearly show an improved boundary layer structure and subsequent CI location and timing when UAV data are added to the control experiment. Through a series of experiments testing various maximum flight levels of the UAVs, it was determined that although flights up to 3 km above ground level (AGL) provided the best analysis of the boundary layer (Figure 4), flights up to 1 km were found to be sufficient in producing an improved CI forecast (Figure 5). On a similar note, a series of network density experiments found that while a UAV network consisting of 110

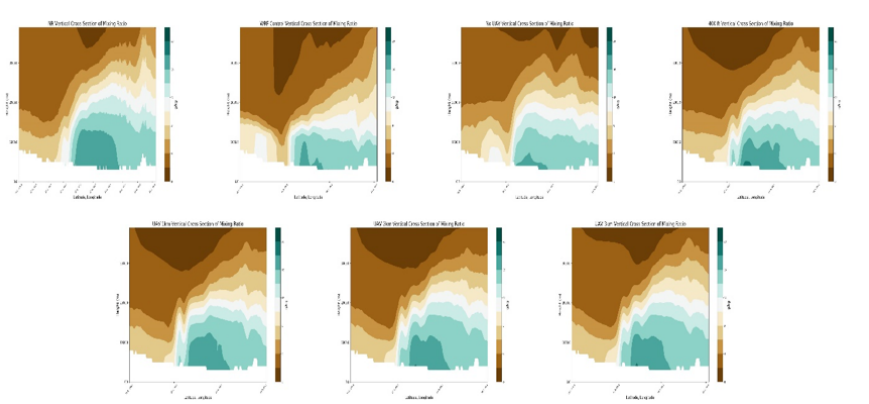


Figure 4. Need better figure from Moore Cross section plots of mixing ratio for the Nature Run (A), WRF Control (B), No UAV (C), UAV 400ft (D), UAV 1km (E), UAV 2km (F), and UAV 3km (G) WRF analyses valid at 1800 UTC 20 May 2013. The Location of the cross section sample is depicted in the upper left image by the black line for reference.

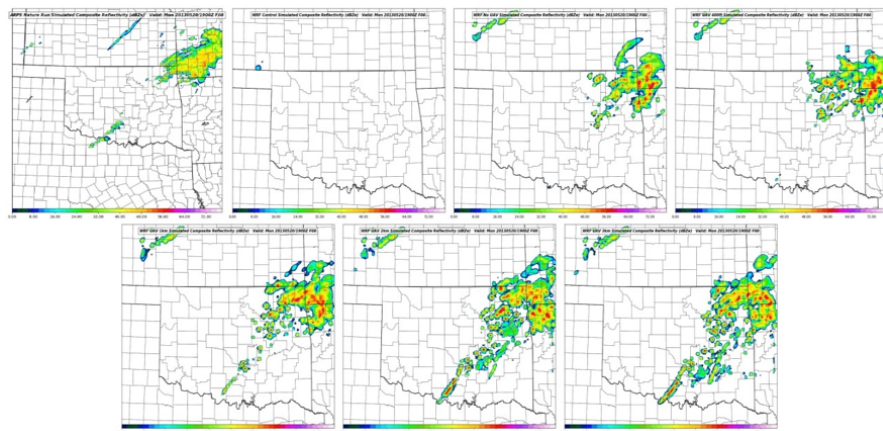


Figure 5. Need better figure from Moore. Comparison between modeled composite radar reflectivity between the Nature Run (A), WRF Control (B), No UAV (C), UAV 400ft (D), UAV 1km (E), UAV 2km (F), and UAV 3km (G) at 1900 on 20 May 2013.

215 UAV stations produced the best results, the CI forecast was improved with only 75 UAV stations.
 216 Although sensitivities to the quality of the moisture analysis are noted, the results suggest that a
 217 real-world deployment of automated UAVs could have a positive impact on atmospheric analyses
 218 and short-term numerical weather prediction of convective initiation.

219 3. Platform and Sensor Development

- 220 • Discuss the design criteria for the UAV
- 221 • Provide a discussion of the current version of the CopterSonde (will this material be discussed in
222 another paper?)
- 223 • Include picture of the CopterSonde (Figure 6)
- 224 • Outline the specifications (Table 1)
- 225 • Mention the target accuracy for the sensors (Table 2)
- 226 • Refer to Greene et al.

227 The general concept of operations for the 3D Mesonet places certain design criteria on the
 228 WxUAS to be used. Flights should be conducted autonomously or semi-autonomously with minimal
 229 human interactions. It should consist of a vertical take-off and landing (VTOL) aircraft for the sake of
 230 docking and charging. This can be achieved using a rotary-wing aircraft or a hybrid vehicle capable



Figure 6. Placeholder: Picture of the CopterSonde

of operating in a rotary-wing mode for take off and landing and then transitioning into a fixed-wing aircraft as its primary mode for data collection. Here we present developments rotary-wing VTOL vehicle using, known as the CopterSonde. Hybrid vehicles are currently under development within CASS and will be presented in forthcoming publications.

The CopterSonde series rotary-wing UAS was developed in-house by a CASS team of engineers and meteorologists to be both robust and optimized for atmospheric sampling. True to its name, the platforms are able to collect vertical profiles of the atmosphere like a traditional radiosonde or ozonesonde. However, these platforms provide highly resolved data (<10 m) in the lower atmosphere that are not easily achievable using conventional methods. The team will be deploying two different models of the CopterSonde platform: one rotary-wing platform designed for thermo-kinematic profiling (CopterSonde 2), and another developed for chemistry profiling (CopterSonde 3). They are also both designed to be weather resistant and can comfortably operate in 40 knot winds.

The CopterSonde 2 (Figure 6) is based on the HQuad500 manufactured by Lynxmotion. It is comprised of carbon fiber plates, aluminum brackets, and carbon fiber tube legs. The rotary-wing craft is electrically powered by four identical brushless motors with T-style carbon fiber propellers. A lithium polymer battery pack with a capacity of 6750 mAh provides a maximum flight endurance of 25 minutes and can allow the platform to climb to a maximum altitude of 6000 ft ASL. The electronic components are protected from the elements with a custom 3D printed two-piece plastic shell, which was designed to enhance the vehicle's aerodynamics and allow for easy access to the interior components.

All CopterSonde platforms utilize open-source technologies to enable autonomous operation of the vehicle. The first of these is a Pixhawk 2.1 flight controller (ProfiCNC), which is comprised of a rugged and vibrationally isolated microcontroller interfaced with a carrier board that allows for communication with a large variety of sensors over a wide range of communication protocols (I2C, UART, RS232, etc.) When paired with the Here+ GPS module (ProfiCNC), the Pixhawk is able to utilize Real Time Kinematic (RTK) GPS, which can reduce the uncertainty of the location of the UAS to less than 1 m in both the horizontal and vertical if properly set-up and calibrated. The microcontroller runs the ArduPilot autopilot software suite, which is composed of navigation software onboard the vehicle and ground station software that is transmitting commands to the UAS over telemetry link.

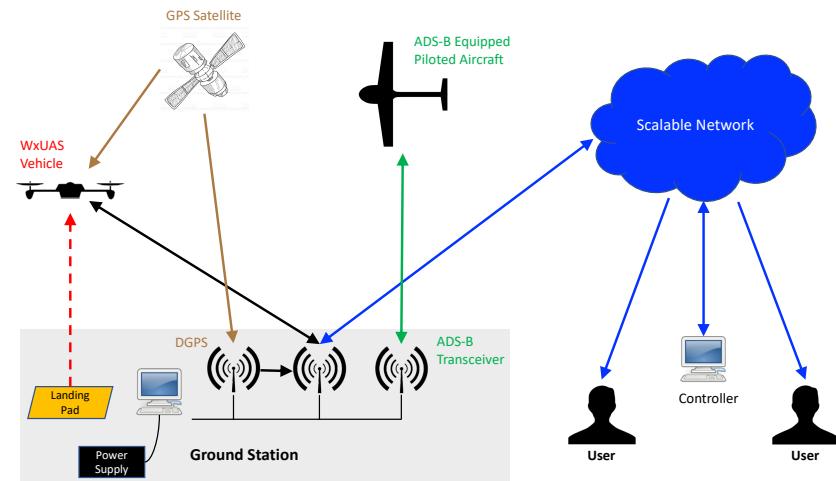


Figure 7. Placeholder: Graphic of how the components of the ground station are linked

When used with the flight controller, it creates a highly customizable environment that can be used to dictate the sampling speed of the sensors, flight path of the vehicle, ascent rate, and much more.

The CopterSonde 2 will be equipped with three Innovative Sensor Technology HYT humidity sensors, three InterMet Bead Thermistors, and a MS5611 Barometer to measure pressure. The temperature and humidity sensors are located on the front of the vehicle in the 3D printed scoop designed to protect the sensors from solar radiation and serve as the front half of the platform's protective shell. A ducted fan is placed in the bottom of the scoop and used to aspirate the sensors by pulling air over them at a constant rate. The barometer is located inside of the autopilot. Wind velocity and direction is calculated using an ardupilot based algorithm that uses the pitch, yaw, and roll angle of the platform. Additionally, the rotary-wing craft uses the results of the wind algorithm to keep the vehicle facing into the wind as to allow for sampling of air undisturbed by the propellers.

4. Supporting Components of the 3D Mesonet

4.1. Ground Station

- Provide a description of what the ground station should provide
- Show a schematic / graphic of how the components are linked (Figure 7) (Liz comment: Is this the same as Figure 2? Could we combine the figures into one large figure or are you going to create more of a block diagram for 6?)

4.2. Risk Mitigation: GeoFence Radar

- Overview of the role the GeoFence Radar plays to deconflict the NAS (will this material be discussed in another paper?)
- Specifications of the radar (Table 3)
- Picture of the radar at KAEFS (Figure 8)
- How detection and alerts are handled
- Screenshot of an aircraft detection (Figure 9)

The research team has developed technology supporting beyond-visual-line-of-sight (BVLOS) small unmanned aircraft systems (sUAS) operations within a defined airspace volume. The specific goal of demonstrating a low-cost, readily manufactured ground-based detect- and-avoid (GBDAA) radar has been achieved. In particular, a prototype radar has been build in the team's lab at the



Figure 8. Placeholder: Picture of the GeoFence Radar mounted on a tower at KAEFS with an inset picture showing the radar hardware

288 Advanced Radar Research Center (ARRC) at the University of Oklahoma, and aircraft from the
 289 university's Department of Aviation have been flown in specific patterns to confirm radar detections.
 290 The radar's primary specifications are: 5.6 GHz operating frequency, 10 MHz to 20 MHz of operating
 291 bandwidth, 6.3 kW peak transmit power, maximum duty cycle = 10%, range = 5 km, probability
 292 of detection within range = 99.9%. As such, the radar will scan continuously, aiming for a high
 293 probability of detecting targets entering a 5 km range. Power supplies, a processing unit, an antenna,
 294 and radio frequency components for both transmitting and receiving signals have been designed for
 295 the radar. An experimental picture is depicted below.

296 To detect targets, the team implemented an algorithm derived from a traditional Constant
 297 False-Alarm Rate (CFAR) detection algorithm. This algorithm uses radar data to estimate random
 298 noise levels and distinguish targets from noise. While operating, the GBDAA Radar generates
 299 a stream of measurements, each pointed in the current direction of the radar as it spins. Once
 300 the radar completes a full circle, the receiver has assembled a Plan Position Indicator (PPI). The
 301 second component of the program is our CFAR implementation, which plots detections on an
 302 image of the PPI. We were successful in running the program in real time, ideally allowing for
 303 immediate visualization of aircraft within the radar's effective range. The program also saves data
 304 from completed PPIs and periodically stores the resulting visualization for later review. We have
 305 conducted several flight tests. The aircraft target used was a single-engine, four-seater Piper Warrior
 306 III, a common aircraft which served as a type specimen for the light aircraft GBDAA Radar was
 307 designed to detect. This test consisted of a series of maneuvers that aimed to test the capabilities of
 308 the GBDAA Radar. We developed a flight plan which ensured that the radar could view its target at
 309 many different altitudes and ranges.

310 On February 26, 2018, the flight plan began with the plane approaching the location of the radar
 311 from the Max Westheimer Airport. The the Piper Warrior III airplane then proceeded to complete
 312 two figure-eight patterns of 1-mile radius loops. The plane then ascended to 1,500 feet, completed 2
 313 passes over the radar, and ascended to 5,000 feet. The final maneuver of the plan was to complete a
 314 loop 4 miles in radius before returning to the airport. The route of the plan can be seen in Figure 4
 315 below with the initial figure eight in red, the passes overhead in green, and the final loop in yellow.

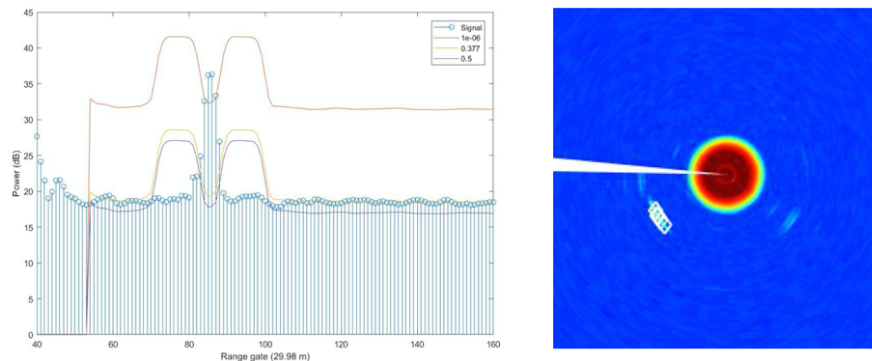


Figure 9. Placeholder: GeoFence Radar screen shot. [Get original file from Yeary](#). Left - detection algorithm performance , Right - several detections forming a track

Specific detections are shown in the figure below. In particular the graph on the left depicts the behavior of the CFAR algorithm. The figure on the right depicts a set of detections in the lower-left quadrant. The right wedge in the left of the figure depicts strong reflections from a nearby water tower.

4.3. Risk Mitigation: ADS-B

- Overview of ADS-B
- Concept of how ADS-B will be used to deconflict the NAS
- Description of our system (we need to hold back because Sai will include this in his paper)
- Screenshot of an aircraft detection and tracking (Figure 10)
- Projection of aircraft path (or leave this out) (Liz comment: I would use this as an opportunity to send them to the new paper)

We used PingStation, an ADS-B receiver from uAvionix. This receiver is a dual band networkable receiver with Power over Ethernet (POE). The PingStation detects ADS-B equipped aircraft within a 240 km (150-mile) radius. The PingStation is robust enough to be used in harsh environmental conditions and small enough to be used as a mobile asset for roaming operations. ADS-B out (ADSB transmission) contain other parameters from the aircraft like altitude, heading, speed and flight number. This information is broadcasted to ADS-B equipped ground stations.

Table 1. Place holder: ADSB specs.

Specification	Value
Input Voltage / Power	44-57 V / 500 mW (Power over Ethernet)
Size	4.75" x 2.0 " x 3.25" (box) 9.5" (antenna)
Weight	340 grams
MTL 1090 MHz	-88 dBm
Dynamic Range	-79 to 0 dBm
MTL 978 MHz	-93 dBm
Dynamic Range	-90 to -3 dBm

Interface is Ethernet (JSON UDP)

So, data from aircraft were obtained using an ADS-B receiver. This data was then sent to a processing computer by configuring Dynamic Host Configuration Protocol (DHCP) connection between receiver and processing computer. Mapbox is a large provider of custom online maps for websites and applications, it allows developers to build applications that are flexible for visualizing geospatial data. In our application we used Mapbox to visualize aircraft trajectories on map. Data received by processing computer is used by Mapbox. A local host connection is used to view

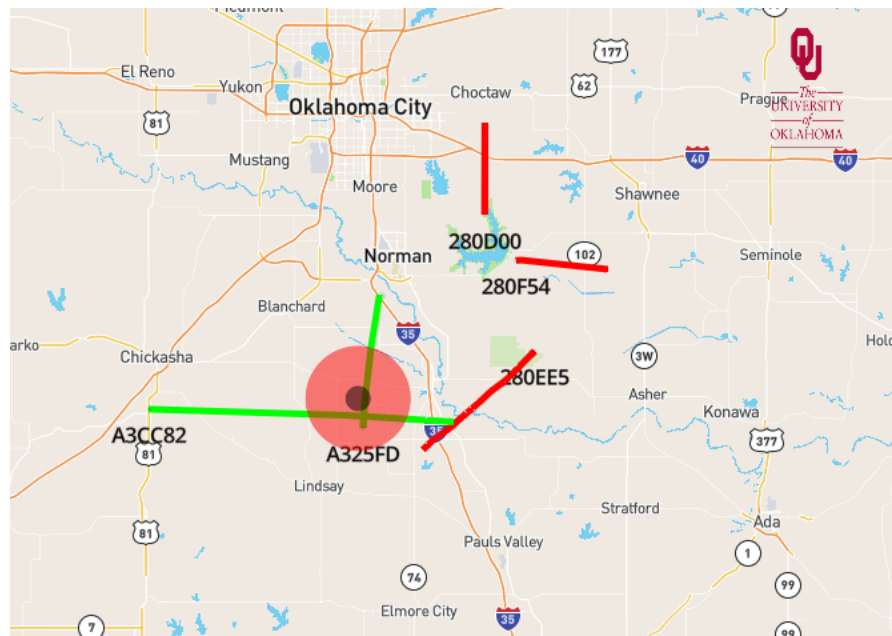


Figure 10. Placeholder: Screen shot of aircraft detection and tracking. Is there a better version of this now?

340 aircraft traffic in the browser. Mapbox together with HTML (Hypertext Markup Language) enable
 341 visualization of air traffic on the map. Air traffic on the map gets updated for every two seconds.
 342 This application was implemented in Python v3.6.

343 5. Data Processing, Distribution, and Visualization

344 5.1. Data Processing and Distribution

- 345 • Discuss data processing on the copter, on the ground station computer, and on the central
 346 processing computer
- 347 • Discuss how data are streamed to/from the copter and ground station and data are streamed
 348 to/from the ground station and cloud and data are streamed to/from the cloud and central
 349 processing computer
- 350 • Show a schematic / graphic of the data flow (Figure 11)

351 5.2. Data Visualization

- 352 • Mention the real time display on the ground station
- 353 • Discuss the real time display on remote servers
- 354 • Show a screenshot of the display (Figure 12)
- 355 • Outline how computation of data visualization will be distributed

356 5.3. Data Examples

- 357 • Provide some examples of data collection from various field experiments (Liz comment: Could
 358 be an opportunity to say that we have worked in both extremes and the knowledge we gained
 359 will make it easier for us to make our system rugged enough to deal with OK extremes.)
- 360 • Show a skew-T log-p plot for one sounding (Figure 13)
- 361 • Show a time-height plot of temperature and dew-point temperature (or similar) (Figure 14)
- 362 • Discuss the value of having such data

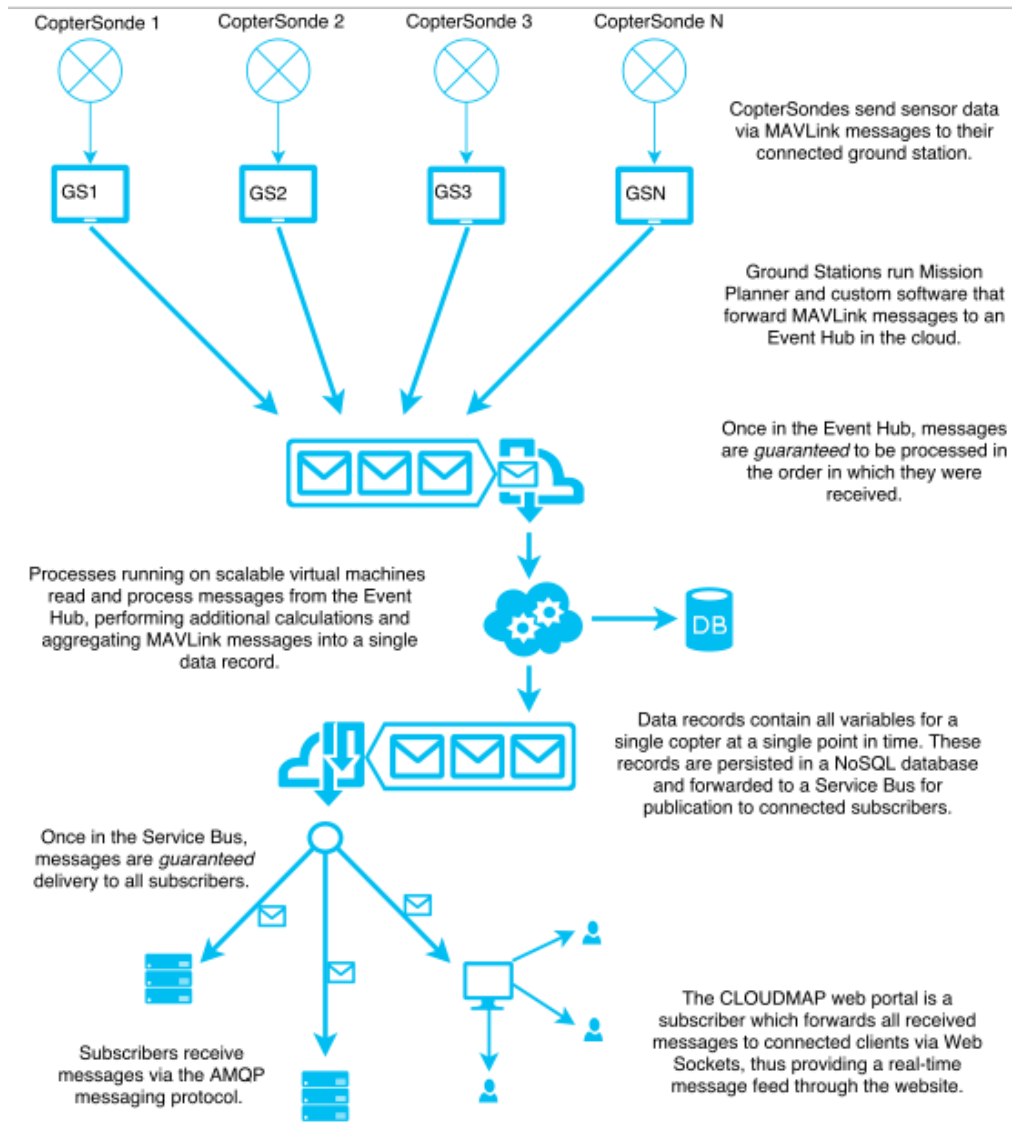


Figure 11. Placeholder: Graphic depicting the data flow **Is this still correct? Can the figure be simplified?**



Figure 12. Placeholder: Screen shot of the ground station [Get from Brian Greene](#).

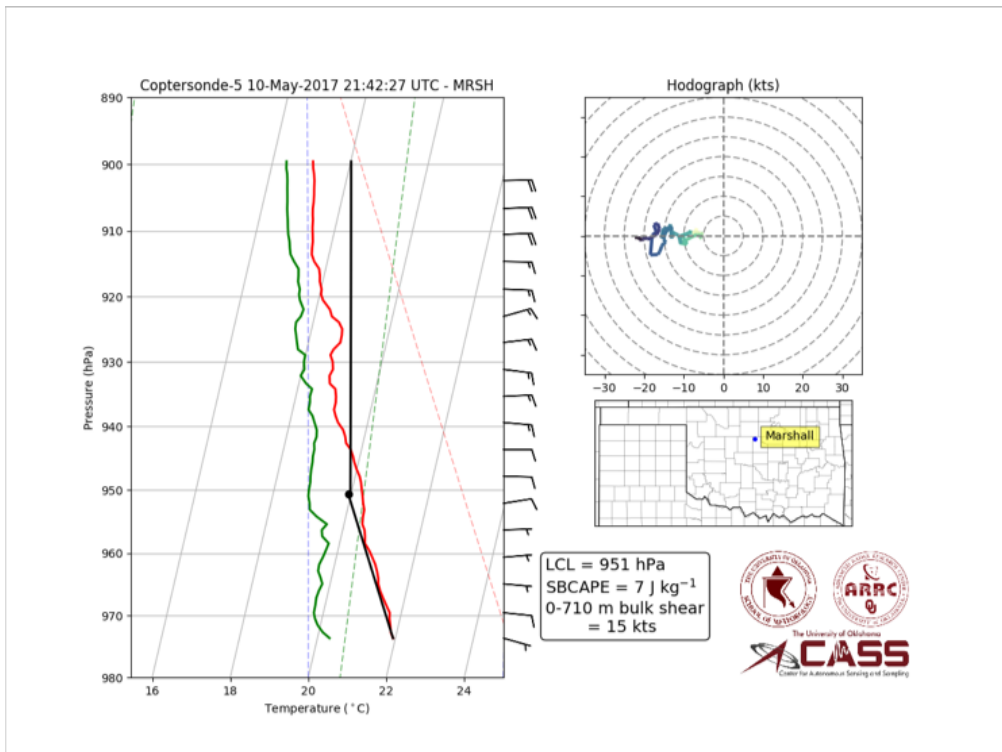


Figure 13. Placeholder: skew T log p plot. [Get revised version from Brian Greene.](#)

363 6. Future Directions

- 364 • Continue to harden and automate the system
- 365 • Establish a small prototype network
- 366 • Continue to evaluate the value of the measurements via OSSEs
- 367 • Begin assimilating data into forecast models

368 7. Conclusions

- 369 • Networks of WxUAS observations could help to fill the measurement gap in the lower atmosphere
- 370 • The technology is available but we need to address regulatory issues (Liz comment: Good
- 371 opportunity to highlight the partnership we have with the Choctaw IPP and other COA successes
- 372 we have.)
- 373 • Data provided by such a network could have a significant impact on weather forecasts and overall
- 374 situational awareness of impending weather developments

375 **Supplementary Materials:** The following are available online at www.mdpi.com/link, Figure S1: title, Table S1: title, Video S1: title.

377 **Acknowledgments:** All sources of funding of the study should be disclosed. Please clearly indicate grants that

378 you have received in support of your research work. Clearly state if you received funds for covering the costs to

379 publish in open access.

380 **Author Contributions:** For research articles with several authors, a short paragraph specifying their individual

381 contributions must be provided. The following statements should be used “X.X. and Y.Y. conceived and

382 designed the experiments; X.X. performed the experiments; X.X. and Y.Y. analyzed the data; W.W. contributed

383 reagents/materials/analysis tools; Y.Y. wrote the paper.” Authorship must be limited to those who have

384 contributed substantially to the work reported.

385 **Conflicts of Interest:** Declare conflicts of interest or state “The authors declare no conflict of interest.” Authors

386 must identify and declare any personal circumstances or interest that may be perceived as inappropriately

387 influencing the representation or interpretation of reported research results. Any role of the funding sponsors

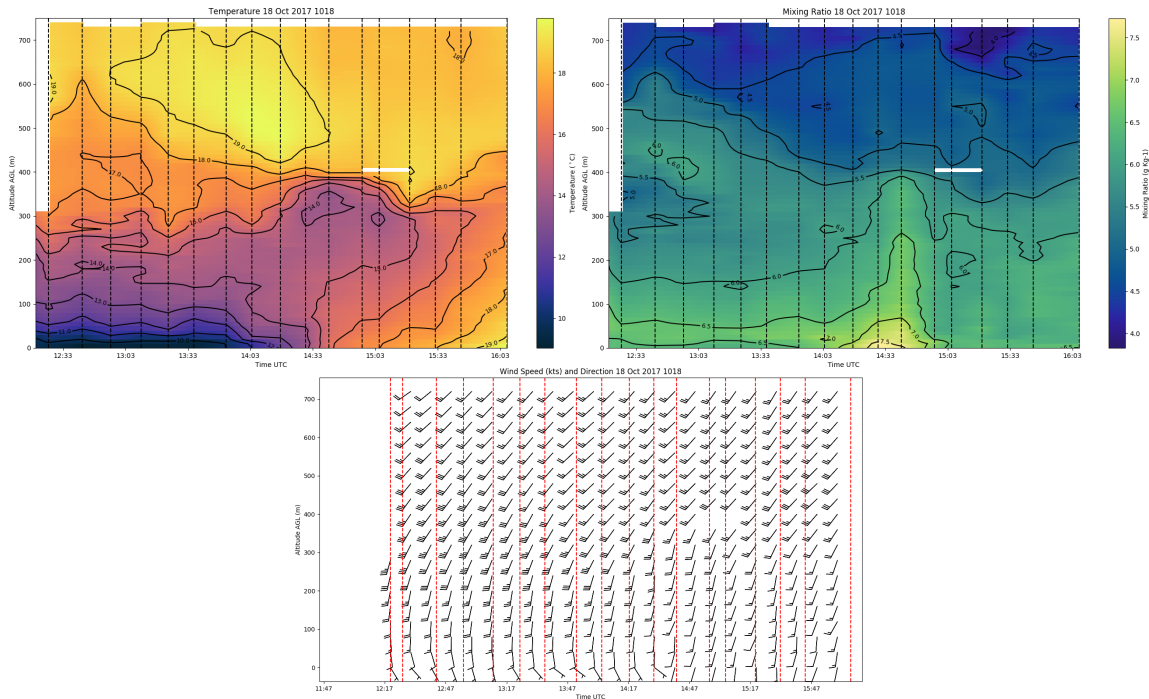


Figure 14. Time-height profiles from data collected using a profiling WxUAS. *Maybe a different plot. If we use these increase the axes labels.*

in the design of the study; in the collection, analyses or interpretation of data; in the writing of the manuscript, or in the decision to publish the results must be declared in this section. If there is no role, please state "The founding sponsors had no role in the design of the study; in the collection, analyses, or interpretation of data; in the writing of the manuscript, and in the decision to publish the results".

392 Bibliography

- 393 1. Lazo, J.K.; Lawson, M.; Larsen, P.H.; Waldman, D.M. U.S. economic sensitivity to weather variability. *Bull. Amer. Meteorol. Soc.* **2011**, *6*, 709–720.
- 394 2. Bloesch, J.; Gourio, F. The effect of winter weather on U.S. economic activity. *Econ. Perspectives* **2015**, *39*, 1–20.
- 395 3. World Meteorological Organization. WMO Statement on the State of the Global Climate in 2017. Technical Report WMO-No. 1212, World Meteorological Organization, 2018.
- 396 4. National Research Council, Washington, D. *Observing Weather and Climate from the Ground Up: A Nationwide Network of Networks*; National Academy Press, 2009.
- 397 5. Hardesty, R.M.; Hoff, R.M. Thermodynamic Profiling Technologies Workshop Report to the National Science Foundation and the National Weather Service. Technical Report NCAR/TN-488+STR, National Center for Atmospheric Research, 2012.
- 398 6. National Academies of Sciences, Engineering, and Medicine. *Thriving on Our Changing Planet: A Decadal Strategy for Earth Observation from Space*; The National Academies Press: Washington, DC, 2018.
- 399 7. National Academies of Sciences, Engineering, and Medicine. *The Future of Atmospheric Boundary Layer Observing, Understanding, and Modeling: Proceedings of a Workshop*; The National Academies Press: Washington, DC, 2018.
- 400 8. Geerts, B.; Raymond, D.; Barth, M.; Detwiler, A.; Klein, P.; Lee, W.C.; Markowski, P.; Mullendore, G. Community Workshop on Developing Requirements for In Situ and Remote Sensing Capabilities in Convective and Turbulent Environments (C-RITE). Technical report, UCAR/NCAR Earth Observing Laboratory, 2017.

- 413 9. Dabberdt, W.F.; Schlatter, T.W.; Carr, F.H.; Friday, E.W.J.; Jorgensen, D.; Koch, S.; Pirone, M.; Ralph, F.M.;
414 Sun, J.; Welsh, P.; Wilson, J.W.; Zou, X. Multifunctioning mesoscale observing networks. *Bull. Amer.*
415 *Meteorol. Soc.* **2005**, *86*, 961–982.
- 416 10. Mahmood, R.; Boyles, R.; Brinson, K.; Fiebrich, C.; Foster, S.; Hubbard, K.; Robinson, D.; Andresen, J.;
417 Leathers, D. Mesonets: Mesoscale weather and climate observations for the United States. *Bull. Amer.*
418 *Meteorol. Soc.* **2017**, *98*, 1349–1361.
- 419 11. Ziokowska, J.R.; Fiebrich, C.A.; Carlson, J.D.; Melvin, A.D.; Sutherland, A.J.; Kloesel, K.A.; McManus,
420 G.D.; Illston, B.G.; Hocker, J.E.; Reyes, R. Benefits and beneficiaries of the Oklahoma Mesonet: A
421 multisectoral ripple effect analysis. *Weather Climate Soc.* **2017**, *9*.
- 422 12. Teixeira, J.; Stevens, B.; Bretherton, C.S.; Cederwall, R.; Klein, S.A.; Lundquist, J.K.; Doyle, J.D.; Golaz,
423 J.C.; Holtslag, A.A.M.; Randall, D.A.; Randall, A.A.; Soares, P.M.M. Parameterization of the atmospheric
424 boundary layer: A view from just above the inversion. *Bull. Amer. Meteorol. Soc.* **2008**, *89*, 553–458.
- 425 13. Markowski, P.M.; Straka, J.M.; Rasmussen, E.N.; Blanchard, D.O. Variability of storm-relative helicity
426 during VORTEX. *Mon. Wea. Rev.* **1998**, *126*, 2959–2971.
- 427 14. Coffer, B.E.; Parker, M.D. Simulated supercells in nontornadic and tornadic VORTEX2 environments.
428 *Mon. Wea. Rev.* **2017**, *145*, 149–180.
- 429 15. McPherson, R.A.; Fiebrich, C.A.; Crawford, K.C.; Kilby, J.R.; Grimsley, D.L.; Martinez, J.E.; Basara, J.B.;
430 Illston, B.G.; Morris, D.A.; Kloesel, K.A.; Melvin, A.D.; Shrivastava, H.; nbarger, J.M.W.; Bostic, J.P.;
431 Demko, D.B.; Elliott, R.L.; Stadler, S.J.; Carlson, J.; Sutherland, A.J. Statewide Monitoring of the Mesoscale
432 Environment: A Technical Update on the Oklahoma Mesonet. *J. Atmos. Ocean. Tech.* **2007**, *24*, 301–321.
- 433 16. Xue, M.; Droege, K.; Wong, K. The advanced regional prediction system (ARPS) - A multi-scale
434 nonhydrostatic atmospheric simulation and prediction model. Part 1: Model dynamics and verification.
435 *Meteorol. Atmos. Phys.* **2000**, *75*, 161–193.

436 © 2018 by the authors. Submitted to *Sensors* for possible open access publication under the terms and conditions
437 of the Creative Commons Attribution license (<http://creativecommons.org/licenses/by/4.0/>)